Journal of King Saud University – Science 35 (2023) 102478

HOSTED BY

Contents lists available at ScienceDirect

Journal of King Saud University – Science

journal homepage: www.sciencedirect.com

Original article

Exploring the therapeutic potential of GC–MS separated compounds from Dracaena cinnabari against dengue virus and *Aedes aegypti* using in silico tools

Nael Abutaha [1], Bader O. Almutairi [1,*]

Department of Zoology, College of Science, King Saud University, P.O. Box 2455, Riyadh 11451, Riyadh, Saudi Arabia

ARTICLE INFO

Article history:
Received 24 July 2022
Revised 25 September 2022
Accepted 29 November 2022
Available online 7 December 2022

Keywords:
Gas chromatography
Aedes aegypti
Dengue virus
Dracaena cinnabari
Molecular docking
Drug-likeness

ABSTRACT

The paper's main aim was to investigate bioactive molecules in *Dracaena cinnabari* extract using gas chromatography-mass spectroscopy (GC–MS) and to assess their therapeutic potential using molecular docking algorithm, ProTox II and ADME studies on dengue virus and *Aedes aegypti*. Molecular docking was carried out using AutoDock Vina, followed by drug-likeness potential and toxicity using in silico tools (ProTox II and ADME). A total of 25 different compounds were detected in the methanol extract, and the major compounds were *cis*-13-Octadecenoic acid (19.04 %), *n*-Hexadecanoic acid (16.5 %), beta-Sitosterol (10.5 %), and *n*-Heptadecanol-1 (9.74 %). Molecular docking revealed that beta-Sitosterol and stigmasterol are the lead compounds and scored the highest docking value among the compounds. The best-docked ligand score for dengue virus was recorded for 4V0Q (stigmasterol, −9.0 kcal/mol), whereas the best-docked ligand score for *Ae. agypti* was recorded for 1PZ4 (beta-Sitosterol, −9.9 kcal/mol). The toxicity prediction for the beta-Sitosterol and 4,4′-Dihydroxy-2 methoxydihydrochalcone did not violate the Lipinski rules. The values of LD_{50} predicted using ProTox II revealed that stigmasterol, 4,4′-dihydroxy-2-methox ydihydrochalcone, beta-Sitosterol, and vitamin E ranged from 890 to 5000 mg kg − 1 in a rat model. This study depicts the potential of promising molecules of *D. cinnabari*. However, in vivo and in vitro investigation is needed to support the results of this study.

1. Introduction

Dengue fever is an infection caused by the dengue virus (DENV) and transmitted through the bite of infected mosquitoes. The number of dengue cases reported increased over 8-fold from 2000 (505,430 cases) to over 2.4 million in 2010 and 5.2 million in 2019 (WHO, 2022). It is estimated that about 60 % of the world population will be at risk of Dengue fever in 2080 (Messina et al., 2019). In Makkah, Saudi Arabia, dengue cases have increased in recent years. The incidence of dengue cases was 204, 163 and 748 in 2017, 2018 and 2019, respectively. In Makkah, the density of Aedes mosquitoes was higher in 2019 with respect to 2017 and 2018. *Ae. albopictus* has not been reported to be present in Makkah; therefore, *Ae. aegypti* is thought to be the principal vector for dengue spread (Sami et al., 2021).

Although all the stages of the DENV replication cycle are prone to inhibition (Magden et al., 2005), no drug is licensed for use in infected patients. Therefore, research, development and assessment in this area are vital. Since vector control is the primary tool for controlling arboviruses, investment in research to combat Ae. aegypti is also growing (Geris et al., 2012). Several methods are already used to combat viruses (Goldenthal et al., 1996) and mosquitoes (Benelli 2015). However, antiviral and insecticidal agents derived from natural products offer a promising source of safer new products for viral and mosquito control due to minimal side effects and residues, therefore minimizing ecosystem disruption (Seo et al., 2012). There is considerable research on antiviral and insecticides of natural origin, especially of botanical origin, due to their innumerable secondary metabolites produced mainly as a defence mechanism against natural predators (Williams et al., 1989).

* Corresponding author.
E-mail address: bomotairi@ksu.edu.sa (B.O. Almutairi).
[1] These two authors contributed equally to this work.
Peer review under responsibility of King Saud University.

Production and hosting by Elsevier

https://doi.org/10.1016/j.jksus.2022.102478

Dracaena cinnabari (common name: Dragon's blood) is a 30–60 feet tall tree that belongs to the Agavaceae family. The family Agavaceae comprises over 100 genera distributed in subtropical and tropical regions. The dragon's blood tree is famous for the red sap that oozes out of it when 3injured (Baumer and Dietemann 2010) (Al-Awthan and Bahattab 2021). It has been used traditionally as an analgesic, abortifacient, astringent, antiseptic, hemostatic, antiulcer; and to treat diarrhoea, fevers, fractures, burns (Al-Awthan et al., 2010) (Xin et al., 2011), skin, eye, and dental diseases (Al-Fatimi 2018). Several pharmacological effects have also been reported, such as wound healing, antidiabetic, antimicrobial, anti-inflammatory, antispasmodic, anticancer, antitumor, hypolipidemic, and analgesic relaxant effects (Al-Awthan and Bahattab 2021).

Considering the need to continue searching for specific larvicidal and antivirals from natural sources, this study aimed to explore in silico interactions of secondary metabolites extracted as well as reported in the literature that may open the door for promising compounds as both larvicidal and antiviral agents. Our results revealed that the compounds extracted and reported from *D. cinnabari* are promising secondary metabolites for developing larvicidal and anti-DENV agents.

2. Materials and methods

2.1. Plant extraction

Twenty grams of *D. cinnabari* resin were obtained from Riyadh (Al-Morroj, Riyadh, Saudi Arabia) and pulverized using a commercial blender (SFstardust, Japan). The powder was extracted using methanol (MeOH) in a sonicator (WiseClean, Witeg, China) for 10 mins at 40° C. The methanol (Sigma–Aldrich, MO, USA) extract was filtered using Whatman filter paper number 1 and evaporated using a rotary evaporator (Heidolph, Schwabach, Germany) at 40 °C. The process was repeated twice, and the yield was calculated. The stock solution prepared was kept at 80 °C.

2.2. Analysis of extract by gas chromatography and mass spectrometry (GC–MS)

The chemical constituents of *D. cinnabari* resin MeOH extract were investigated using GC**–MS** (Turbomass, PerkinElmer, MA, USA). HP-88 capillary column (100 m, ID: 250 μm) was used for the study. The temperature was adjusted to 40 °C for a 2 min hold, followed by increasing the temperature to 200 °C (5 °C/min) and held for 2 min. The temperature was later raised to 300 °C (5 °C/min) and held for another 2 min. The phytochemical composition of MeOH extract was investigated by comparing the mass spectra of detected compounds with the Wiley GC–MS Library (McLafferty and Stauffer 1989) and the National Institute of Standard and Technology Spectral Library, the Adams Library (Adams 2007).

2.3. Preparation of ligands

The 3D structures of the compounds extracted from the *D. cinnabari* and reported from the literature (Ying et al., 2011, Al-Awthan and Bahattab 2021) were downloaded from the PubChem (https://pubchem.ncbi.nlm.nih.gov/). The structures of *D. cinnabari* compounds in table 1 and table 8 (supplementary material) were converted to "PDBQT" files from "SDF" format using Open Babel v.2.4.0 software (https://sourceforge.net/projects/openbabel/files/openbabel/2.4.0/). The energy-minimized ligands were the input for AutoDock Vina to perform docking simulation.

2.4. Preparation of receptor

AutoDock Vina was used to dock the crystal structural protein (Tables 1 and 2) and isolated compounds (25 compounds) into the active site of the selected target proteins. All the three-dimensional (3D) crystal enzyme structures were downloaded from the Protein Data Bank (PDB) (https://www.rcsb.org). All the associated water molecules and heteroatoms were removed from the original structures, and polar hydrogen atoms were added along with the charges using Auto Dock 4.2 (MGL tools1.5.6) [44]. The grid box was set using Autogrid. Molecules were saved in "PDBQT" format so they could be further processed using AutoDock Vina [45].

2.5. Molecular docking

The algorithm provided with Auto Dock Vina was employed to look for the best-docked conformation between proteins and ligands. The conformations with the lowest free binding energy (ΔG) (best-scored complexes) were selected for the Ligand receptor interaction analysis by PyMOL and the protein–ligand interaction profiler (PLIP).

2.6. In silico pharmacokinetic study

Adsorption, distribution, metabolism, and excretion (ADME) are necessary to analyze the pharmacodynamics attributes of the promising compounds. Chemical notation of the ligands (SMILES) was copied from PubChem (https: //pubchem.ncbi.nlm.nih.gov/compound, accessed on 5 June 2021) and used as an input for SWISS-ADME tool (https://www.swissadme.ch, accessed on 23 June 2022) to predict lipophilicity (Log P0/w, iLOGP, SILICOS-IT, XLOGP3, MLOGP, WLOGP), water solubility-Log S (SILICOS-IT, ESOL, Ali), and drug-likeness rules (Muegge, Veber, Ghose, Lipinski, Ghose, and, Egan,). Toxicology prediction is essential to predict the toxicity of ligands. ProTox-II provides details of various predicted toxicity endpoints such as immunotoxicity, mutagenicity, carcinogenicity, hepatotoxicity, cytotoxicity and acute toxicity. ProTox-II was logged on using SMILES of the compounds, and toxicity mode was assessed.

Table 1
Potential target *Ae. aegypti* proteins and PDB ID used in this study.

No.	Protein	PDB ID
1	Sterol Carrier Protein-2	**2QZT**
2	kynurenine aminotransferase	**1YIY**
3	sterol carrier protein-2	**1PZ4**
4	FKBP12 Isomerase	**3UQI**

Table 2
Potential target DENV1viral proteins and PDB ID used in this study.

No.	Protein	PDB ID
1	DENV1-E111	**4FFY**
2	NS2B/NS3 Protease	**2FOM**
3	Dengue 4 Envelope protein domain III	**3WE1**
4	NS5 RNA dependent RNA polymerase	**2J7U**
5	RNA helicase	**2BMF**
6	RNA-directed RNA polymerase (NS5)	**4V0Q**
7	non-structural protein 1(NS1) chain A	**4O6B**

3. Result

3.1. GC–MS of methanol extract

A total of 25 different compounds were present in the MeOH extract (Table 3). The reported compounds were represented in order of their elution. The major compounds were *cis*-13-Octadecenoic acid (19.04 %), *n*-Hexadecanoic acid (16.5 %), beta-Sitosterol (10.5 %), *n*-Heptadecanol-1 (9.74 %). The remaining compounds are present in small amounts such as Hexadecenoic acid, Z-11- (0.59 %), 1,2-Benzenedicarboxylic acid, diisooctyl ester (0.60 %) and Campesterol (0.71 %).

3.2. Docking studies

Molecular docking was carried out to predict the complex formation between the dengue virus and *Ae. aegypti* target proteins and twenty-five ligands detected in the GC–MS. Ligands showed differences in binding affinity values and the numbers of hydrophobic and hydrogen bonds for their interaction with the target proteins. The results have revealed 2 compounds that docked strongly to dengue virus nonstructural protein (DENV-NS1) and RNA-directed RNA polymerase (DENV-NS5). Similarly, 3 compounds also docked strongly to *Ae. aegypti* Sterol Carrier Protein-2 (1PZ4, 2QZT).

3.3. Screening of inhibitors for 4V0Q

With RNA-directed RNA polymerase (DENV-NS5), ligands stigmasterol, and 4,4′-dihydroxy-2-methoxydihydrochalcone showed binding affinities of − 9.0 and − 8.8 kcal/mol, respectively (Table 3). Further analyses of binding sites between the ligands-DENV-NS5 complexes revealed different binding positions of stigmasterol and 4,4′-dihydroxy-2-methoxydihydrochalcone on the DENV-NS5

Table 3
Binding affinity energies (kcal/mol) of GC–MS isolated compounds against 4FFY, 2FOM, 3WE1, 2J7U, 2BMF, 4V0Q, and 4O6B as viral target sites.

Sr. No.	Name	Molecular weigh	Molecular formula	Area %	4FFY	2FOM	3WE1	2J7U	2BMF	4V0Q	4O6B
1	Camphene	136.125	$C_{10}H_{16}$	1.029234	−5.6	−4.9	−5.2	−5.0	−5.2	−5.1	−4.8
2	Ethanone, 1-(2-methylcyclopropyl)-	98.073	$C_6H_{10}O$	0.910577	−4.1	−4.3	−4.0	−3.8	−4.1	−4.2	4.5
3	Tetradecanoic acid	228.209	$C_{14}H_{28}O_2$	0.775554	−3.8	−5.3	−3.3	−4.6	−5.2	−5.2	−4.7
4	Butanoic acid, 3-methyl-, 3,7-dimethyl-6-octenyl ester	240.209	$C_{15}H_{28}O_2$	1.974359	−4.5	−5.5	−4.8	−4.9	−5.6	−5.7	−4.3
5	*n*-Heptadecanol-1	256.277	$C_{17}H_{36}O$	9.748447	−3.8	−4.6	−3.4	−4.3	−5.1	−4.5	−4.5
6	Hexadecanoic acid, methyl ester	270.256	$C_{17}H_{34}O_2$	1.378555	−3.9	−4.7	−3.3	−4.5	−5.1	−4.8	−6.0
7	7,9-Di-*tert*-butyl-1-oxaspiro(4,5)deca-6,9-diene-2,8-dione	276.173	C17H24O3	2.846544	−6.1	−6.9	–	−6.6	−6.1	−7.1	−3.9
8	Hexadecenoic acid, Z-11-	254.225	$C_{16}H_{30}O_2$	0.593962	−4.0	−5.4	−3.9	−5.3	−5.0	−5.2	−4.0
9	*n*-Hexadecanoic acid	256.24	$C_{16}H_{32}O_2$	16.53734	−3.9	−5.1	−3.9	−5.1	−5.2	−5.4	−4.5
10	1,7-Octadiene, 2,7-dimethyl-3,6-bis(methylene)-	162.141	$C_{12}H_{18}$	2.489961	−4.5	−5.4	−4.5	−4.7	−5.2	−5.2	−4.5
11	1,5-Heptadiyne	92.063	C_7H_8	7.026721	−3.8	−3.9	−3.7	−4.2	−3.8	−4.4	−4.0
12	Naphthalene, 1,2,3,4,4a,5,6,8a-octahydro-4a,8-dimethyl-2-(1-methylethenyl)-, [2R-(2.alpha.,4a.alpha.,8a.beta.)]-	204.188	$C_{15}H_{24}$	4.87512	−5.8	−7.2	−5.8	−6.2	−5.8	−8.0	−5.8
13	*cis*-13-Octadecenoic acid	282.256	$C_{18}H_{34}O_2$	19.42207	−4.5	−4.9	−3.6	−5.0	−4.4	−4.9	−5.0
14	9,12-Octadecadienoic acid (Z,Z)-	280.24	$C_{36}H_{66}O_4$	1.091124	−3.8	−5.4	−4.3	−5.8	−4.8	−5.4	−5.3
15	1H,5H-Pyrido[3,2,1-*ij*]quinolin-5-one, 2,3-dihydro-6-ethyl-7-hydroxy-	229.11	$C_{14}H_{15}NO_2$	4.528984	−6.5	−7.3	−6.1	−6.6	−6.6	−7.3	−6.1
16	Pentadeca-1,3,7,12,14-pentaen-7-ol-9-one	232.146	$C_{15}H_{20}O_2$	1.121466	−4.9	−5.7	−4.6	−5.8	−6.0	−6.0	−5.2
17	Vitamin E	430.381	$C_{29}H_{50}O_2$	1.625102	−4.9	−7.5	−5.8	−6.1	−8.2	−6.3	−6.3
18	2-Methyl-Z,Z-3,13-octadecadienol	280.277	$C_{19}H_{36}O$	0.758699	−4.3	−5.2	−4.0	−4.8	−5.2	−5.5	−4.5
19	cis,*cis*-7,10,-Hexadecadienal	236.214	$C_{16}H_{28}O$	2.362345	−3.9	−5.3	−3.9	−5.0	−4.9	−5.3	−4.3
20	1,2-Benzenedicarboxylic acid, diisooctyl ester	390.277	$C_{24}H_{38}O_4$	0.604336	−4.3	−6.3	−4.2	−6.1	−5.7	−5.3	−4.7
21	Campesterol	400.371	$C_{28}H_{48}O$	0.712619	−7.3	−7.9	−6.4	−8.3	−7.6	−7.8	−8.1
22	1,3,12-Nonadecatriene	262.266	$C_{19}H_{34}$	2.817368	−3.3	−4.9	−3.9	−4.7	−5.2	−5.0	−4.2
23	Stigmasterol	412.371	$C_{29}H_{48}O$	1.69131	−7.1	−8.2	−6.8	−8.2	−7.3	−9.0	−8.9
24	beta.-Sitosterol	414.386	$C_{29}H_{50}O$	10.58025	−6.8	−7.6	−5.6	−8.2	−6.3	−7.6	−7.8
25	2-Ethylacridine	207.105	$C_{15}H_{13}N$	2.497954	−6.0	−7.0	−6.6	−7.1	−8.0	−7.4	−6.3

Table 4
Binding affinity energies (kcal/mol) of GC–MS isolated compounds against 2QZT, 3UQI, 1YIY and 1PZ4 as mosquito target protein.

Sr. No.	Name	Molecular weigh	Molecular formula	Area %	2QZT	3UQI	1YIY	1PZ4
1	Camphene	136.125	$C_{10}H_{16}$	1.029234	−6.1	−6.3	−5.8	−6.8
2	Ethanone, 1-(2-methylcyclopropyl)-	98.073	$C_6H_{10}O$	0.910577	−4.3	−4.6	−5.0	−4.8
3	Tetradecanoic acid	228.209	$C_{14}H_{28}O_2$	0.775554	−5.7	−5.1	−5.3	−6.6
4	Butanoic acid, 3-methyl-, 3,7-dimethyl-6-octenyl ester	240.209	$C_{15}H_{28}O_2$	1.974359	−6.2	−5.3	−6.2	−7.1
5	*n*-Heptadecanol-1	256.277	$C_{17}H_{36}O$	9.748447	−5.8	−4.7	−5.0	−6.4
6	Hexadecanoic acid, methyl ester	270.256	$C_{17}H_{34}O_2$	1.378555	−5.8	−4.2	−5.3	−6.8
7	7,9-Di-*tert*-butyl-1-oxaspiro(4,5)deca-6,9-diene-2,8-dione	276.173	C17H24O3	2.846544	−7.4	−6.6	−7.6	−5.3
8	Hexadecenoic acid, Z-11-	254.225	$C_{16}H_{30}O_2$	0.593962	−6.6	−4.6	−5.6	−6.9
9	*n*-Hexadecanoic acid	256.24	$C_{16}H_{32}O_2$	16.53734	−6.0	−4.6	−5.9	−6.5
10	1,7-Octadiene, 2,7-dimethyl-3,6-bis(methylene)-	162.141	$C_{12}H_{18}$	2.489961	−6.0	−5.2	−5.9	−6.6
11	1,5-Heptadiyne	92.063	C_7H_8	7.026721	−4.6	−4.5	−4.9	−4.7
12	Naphthalene, 1,2,3,4,4a,5,6,8a-octahydro-4a,8-dimethyl-2-(1-methylethenyl)-, [2R-(2.alpha.,4a.alpha.,8a.beta.)]-	204.188	$C_{15}H_{24}$	4.87512	−8.1	−6.4	−7.3	−6.8
13	*cis*-13-Octadecenoic acid	282.256	$C_{18}H_{34}O_2$	19.42207	−6.2	−4.5	−6.2	−7.1
14	9,12-Octadecadienoic acid (Z,Z)-	280.24	$C_{36}H_{66}O_4$	1.091124	−6.8	−4.6	−6.3	−7.6
15	1H,5H-Pyrido[3,2,1-*ij*]quinolin-5-one, 2,3-dihydro-6-ethyl-7-hydroxy-	229.11	$C_{14}H_{15}NO_2$	4.528984	−7.6	−6.6	−7.4	−5.8
16	Pentadeca-1,3,7,12,14-pentaen-7-ol-9-one	232.146	$C_{15}H_{20}O_2$	1.121466	−6.9	−5.3	−6.6	−7.0
17	Vitamin E	430.381	$C_{29}H_{50}O_2$	1.625102	−9.6	−7.2	−7.1	−5.0
18	2-Methyl-Z,Z-3,13-octadecadienol	280.277	$C_{19}H_{36}O$	0.758699	−6.5	−5.2	−5.5	−7.1
19	cis,*cis*-7,10,-Hexadecadienal	236.214	$C_{16}H_{28}O$	2.362345	−5.9	−5.2	−5.5	−6.9
20	1,2-Benzenedicarboxylic acid, diisooctyl ester	390.277	$C_{24}H_{38}O_4$	0.604336	−7.0	−5.1	−5.9	−4.0
21	Campesterol	400.371	$C_{28}H_{48}O$	0.712619	−7.2	−6.2	−8.0	−6.3
22	1,3,12-Nonadecatriene	262.266	$C_{19}H_{34}$	2.817368	−6.4	−5.4	−5.3	−7.1
23	Stigmasterol	412.371	$C_{29}H_{48}O$	1.69131	−7.1	−7.0	−8.1	−6.7
24	beta.-Sitosterol	414.386	$C_{29}H_{50}O$	10.58025	−6.5	−6.6	−7.6	−9.9
25	2-Ethylacridine	207.105	$C_{15}H_{13}N$	2.497954	−8.6	−6.6	−8.3	−9.7

protein via hydrophobic and hydrogen bond formation. The hydrogen bonds between the ligand and the DENV-NS5 protein stabilize the ligand within the binding residues. The docking result of stigmasterol to DENV-NS5 protein formed two hydrogen bonds (ASP13, VAL132) and six hydrophobic interactions. Similarly, the docking result of 4,4′-dihydroxy-2-methoxydihydrochalcone to DENV-NS5 protein formed 4 hydrogen bond (LEU94, LYS96, VAL97 and GLN351) and 5 hydrophobic interactions (ILE72, LEU94, LYS95, PRO298, and GLN351). The docking complexes were studied in-depth for the interactions of each ligand with the active residues of the DENV-NS5 target protein (Table 5, Fig. 1).

3.4. Screening of inhibitors for 4O6B

Stigmasterol, campesterol and beta.-sitosterol were the 3 ligands with the greatest negative values of binding free energy

Table 5
The best docking results of bioactive ligands with RNA-directed RNA polymerase (PDB ID: 4V0Q) and nonstructural protein 1 (PDB ID: 4O6B) targets.

Sr. No.	compounds	Target	No. of H-bond	Interact residues	No. of Hydrophobic interaction	Interact residues	Binding energy (kcal/mol)
23	Stigmasterol	4V0Q	2	ASP13, VAL132	6	TRP87, LYS105, ASP146, ILE147	−9.0
23	Stigmasterol	4O6B	1	ASP1	7	VAL5,LYS14, PHE20, LYS189, ARG192, VAL194	−8.9
5	4,4′-Dihydroxy-2-methoxydihydrochalcone	4V0Q	4	LEU94, LYS96, VAL97, GLN351	5	ILE72,LEU94, LYS95,PRO298, GLN351	−8.8

(Table 3). With DENV-NS1 protein, ligands stigmasterol (−8.9 kcal/-mol), campesterol (−8.1 kcal/mol) and beta-sitosterol (−7.8 kcal/-mol) showed good to moderate affinity binding. The docking result of Stigmasterol to DENV-NS1 protein formed a hydrogen bond (ASP1) and seven hydrophobic interactions (VAL5, LYS14, PHE20, LYS189, ARG192, VAL194). The docking complexes were studied in-depth with the active residues of the DENV-NS1 target protein (Table 5 and Fig. 1).

3.5. Screening of inhibitors for 1PZ4

The ligands showed different binding free energy values with the target protein of AeSCP2 (PDB code: 1PZ4). Ligands beta-Sitosterol (-9.9), 2-Ethylacridine (-9.7), and (2S)-7, 3′-Dihydroxy-4′-methoxyflavane (-9.7) were the 3 ligands with the greatest negative binding free energy values for complex formation (Table 4). Further analyses of potential binding sites between the ligand-**1PZ4** complexes revealed different binding positions of all 3 peptides on the DENV NS1 protein via hydrogen and hydrophobic bond formation (Table 2). The docking result of beta-Sitosterol to AeSCP2 formed a hydrogen bond (GLY75) and 16 hydrophobic interactions. Similarly, the docking result of 2-Ethylacridine to AeSCP2 formed a hydrogen bond (PHE105) and 9 hydrophobic interactions. Nevertheless, some common binding sites are recognized by ligand at specific amino acid residues on the DENV NS1 structure, including ILE12, LEU102, PHE105, GLN25 and LEU109 (Table 6 and Fig. 2).

3.6. Screening of inhibitors for 2QZT

Vitamin E, 2-Ethylacridine, 7,4′-dihydroxy-8-methylflavone and pinoresinol were the 4 ligands with the greatest negative values of binding free energy for complex formation (Table 4). With Sterol Carrier Protein-2, ligands Vitamin E (−9.6 kcal/mol), 2-Ethylacridine (−8.6 kcal/mol), 7,4′-dihydroxy-8-methylflavone (−8.4 kcal/mol) and Pinoresinol (−8.4 kcal/mol) showed good to moderate affinity binding (Table 4). The docking result of vitamin E to Sterol Carrier Protein-2 formed a hydrogen bond (PRO22) and 17 hydrophobic interactions (ILE10, VAL14, VAL17, ARG23, PHE29, LEU21, VAL44, LEU46, ILE73, VAL80, LEU101, VAL104). The docking complexes were visually inspected in-depth for the interactions of each ligand with the active residues of the 2QZT target protein (Table 6 and Fig. 2).

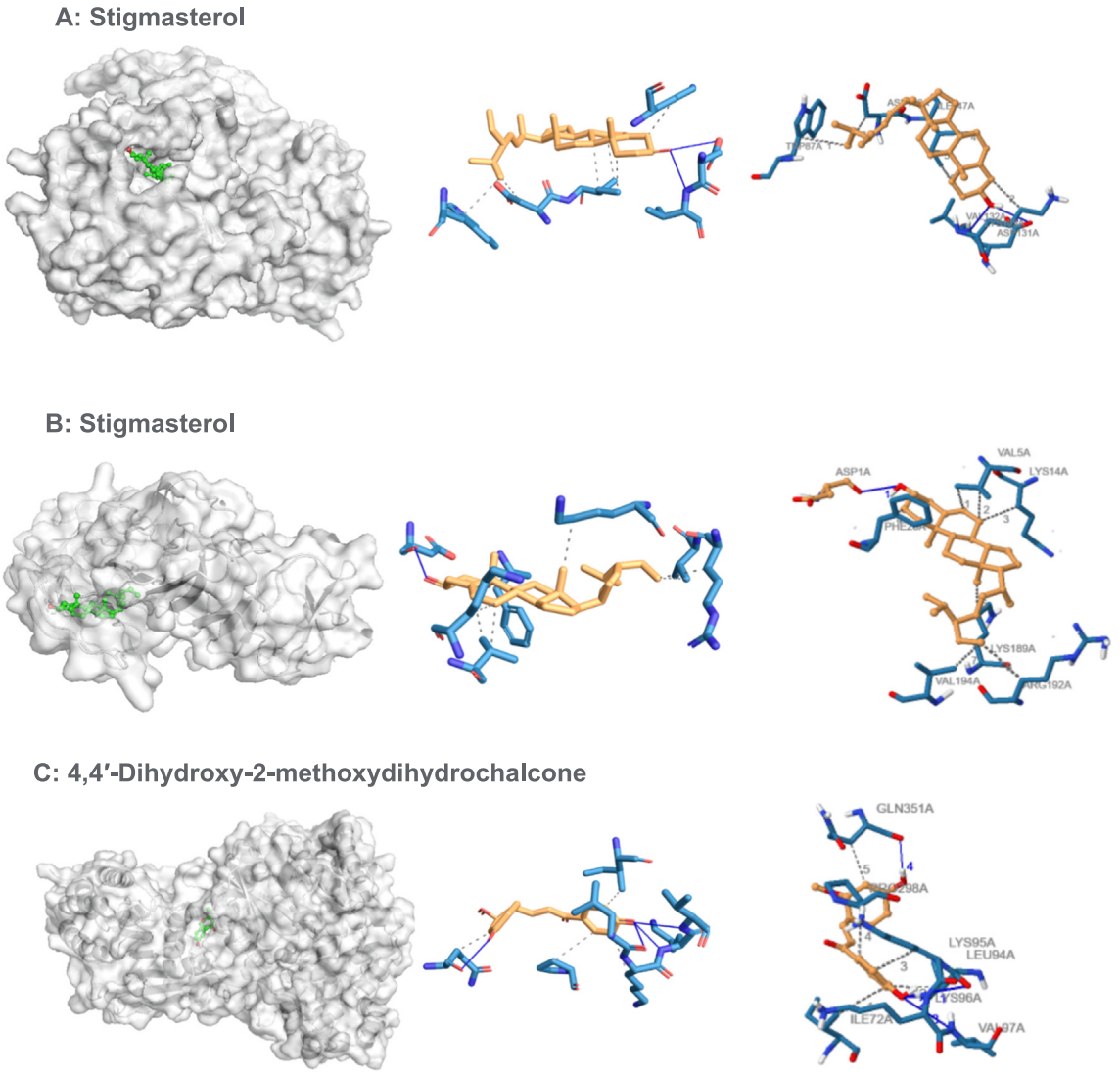

Fig. 1. Binding poses of three top-ranked ligands at the binding site of RNA-directed RNA polymerase (PDB ID: 4V0Q), nonstructural protein 1(NS1) (PDB ID: 4O6B) and 3D and 2D interaction diagrams. (A) Stigmasterol – 4V0Q; (B) Stigmasterol 4O6B; and (C) 4,4′-Dihydroxy-2-methoxydihydrochalcone – 4V0Q.

Table 6
The best docking results of bioactive ligands with sterol carrier protein (PDB ID: 1PZ4 and 2QZT) targets.

Sr. No.	compounds	Target	Interact residues	No. of Hydrophobic interaction	No. of Hydrophobic interaction	Interact residues	Binding energy (kcal/mol)
24	beta.-Sitosterol	1PZ4	1	GLY75A	16	ILE12, ARG15, LEU15, ILE16, ILE19, ARG24, GLN25, VAL36, PHE32,LEU102,PHE105, ILE106, LEU109	−9.9
25	2-Ethylacridine	1PZ4	1	PHE105	9	ILE12, GLN25,VAL26,LEU48, LEU102, PHE105, LEU109	−9.7
17	Vitamin E	2QZT	1	PRO22	17	ILE10, VAL14, VAL 17, ARG23, PHE29, LEU21, VAL44, LEU46, ILE73, VAL80, LEU101, VAL104	−9.6

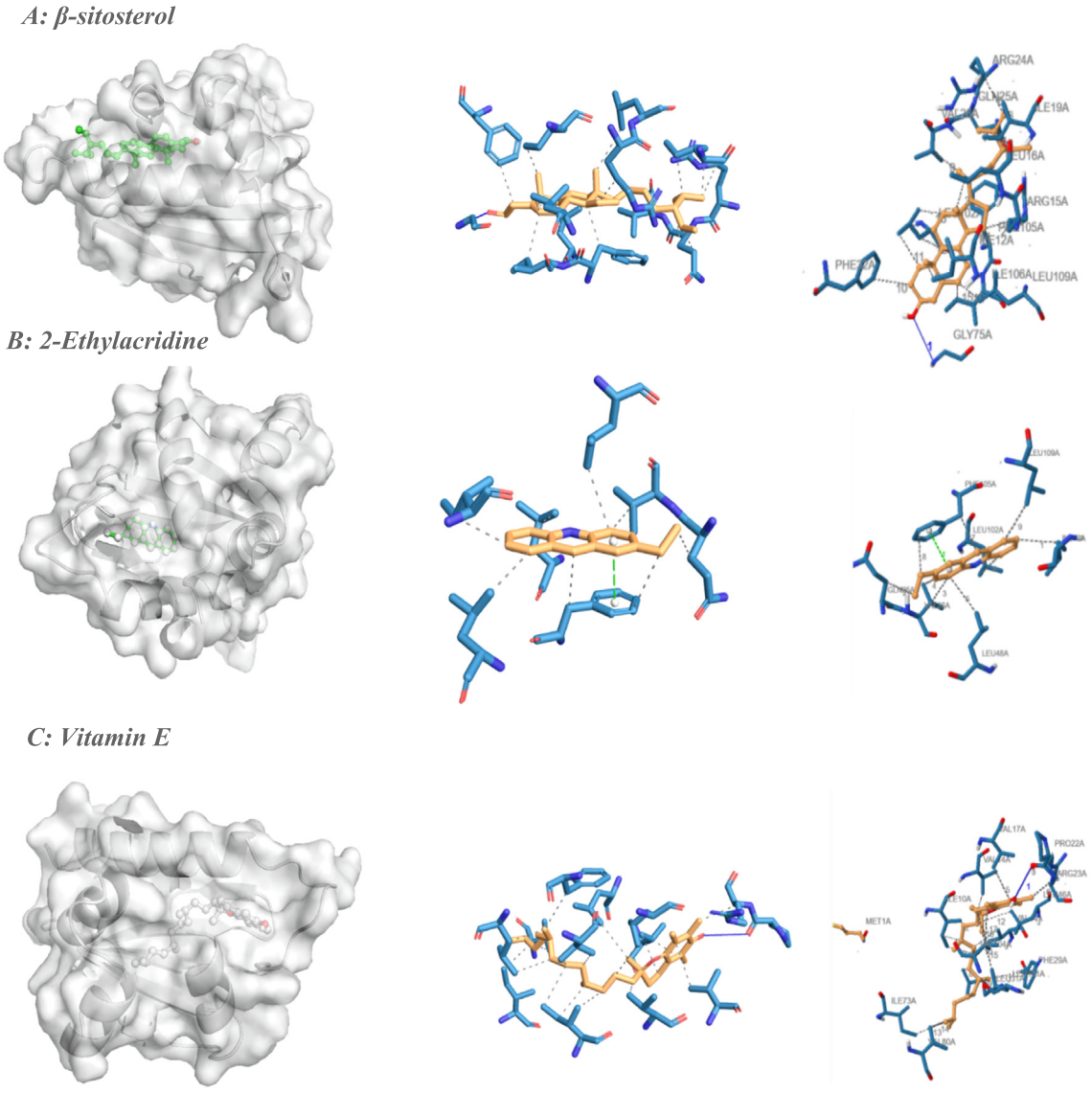

Fig. 2. Binding poses of three top-ranked ligands at the binding site of sterol carrier protein-2 (PDB ID: 1PZ4 and PDB ID: 2QZT) and 3D and 2D interaction diagrams. (A) Stevioside-1PZ4; (B) 2-Ethylacridine −1PZ4; and (C) Vitamin E −2QZT.

3.7. In silico pharmacokinetic study

Promising candidates should have satisfactory ADME properties and be non-toxic. Therefore, the compounds' toxicity and ADME profile were assessed using ProTox II and Swiss ADME approach. The predicted toxicity of selected compounds is shown in Fig. 3 and Table 7. The toxicity prediction for the beta-Sitosterol, and 4,4′-Dihydroxy-2 methoxydihydrochalcone did not violate the Lipinski rules (Fig. 3). The compounds' cytotoxicity, mutagenicity, carcinogenicity and hepatotoxicity have been assessed(Lounkine et al., 2012). Based on the ProTox II result, compound 2-Ethylacridine is mutagenic. Stigmasterol, 4,4′-dihydroxy-2-methoxydihydrochalcone, and beta-Sitosterol are found to be immunotoxic. However, all compounds are not cytotoxic or hepatotoxic. The values predicted LD_{50} using ProTox II revealed that stigmasterol, 4,4′-dihydroxy-2-methoxydihydrochalcone, beta-sitosterol, and

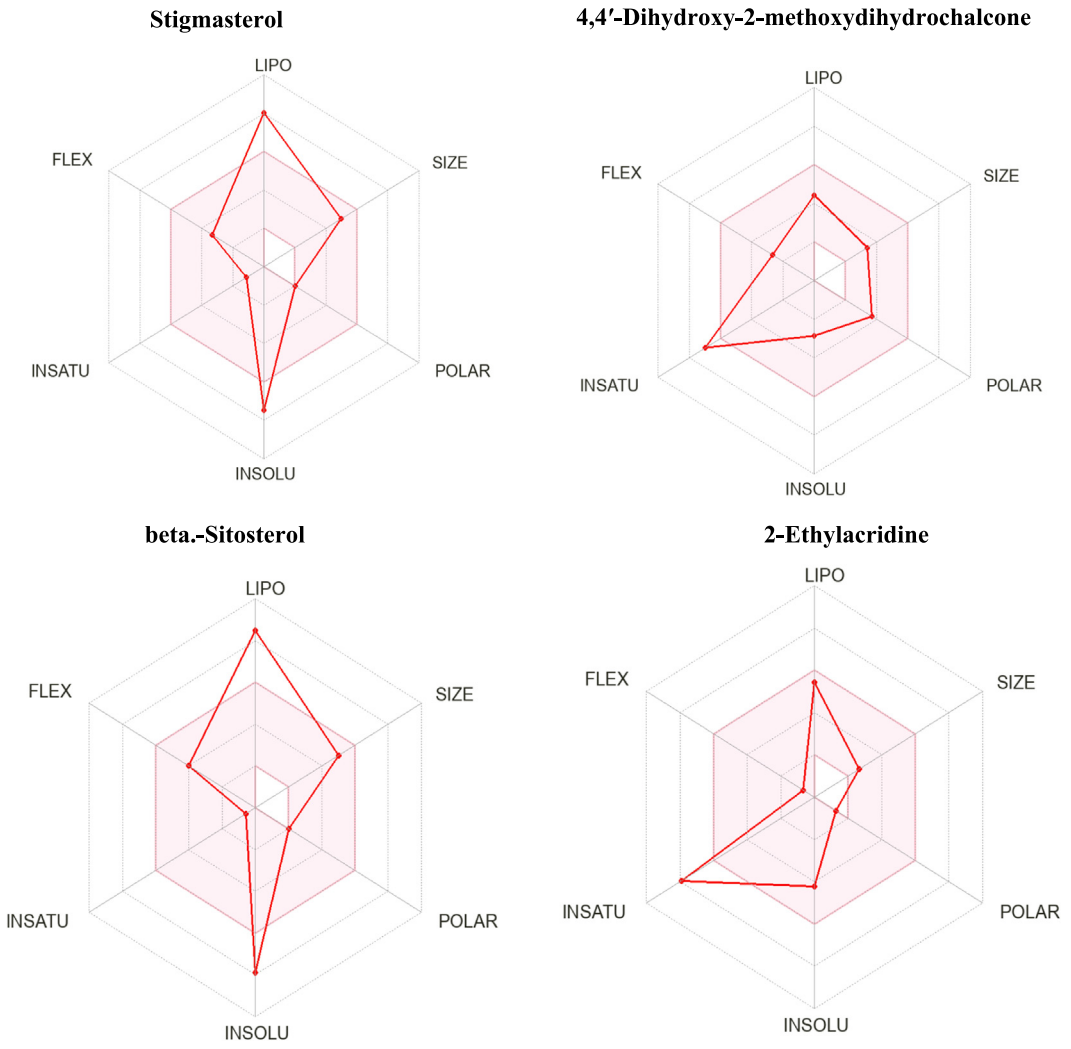

Fig. 3. SwissADME bioavailability radar of the 4 promising drug-likeness ligands, where the pink areas signify each property (FLEX: flexibility, INSOLU: insolubility, LIPO: lipophilicity.

Table 7
Predicted toxicity of the selected compounds using the ProTox-II platform.

Compounds	Predicted:						
	Hepatotoxicity	Carcinogenicity	Immunotoxicity	Mutagenicity	Cytotoxicity	LD_{50} (mg/kg)	Toxicity Class
Stigmasterol	Inactive	Inactive	Active	Inactive	Inactive	890	4
4,4′-Dihydroxy-2-methoxydihydrochalcone	Inactive	Inactive	Active	Inactive	Inactive	1000	4
beta-Sitosterol	Inactive	Inactive	Active	Inactive	Inactive	890	4
2-Ethylacridine	Inactive	Inactive	Inactive	Active	Inactive	940	4
Vitamin E	Inactive	Inactive	Inactive	Inactive	Inactive	5000	5

vitamin E range from 890 to 5000 mg kg − 1 in the rat model (Table 7).

4. Discussion

Computational chemistry plays a substantial role in the drug development process. Virtual screening is widely utilized to reduce the cost and time of drug development. Molecular docking is a technique used to discover novel ligands for target proteins and plays a significant role in structure-based drug design (Kitchen et al., 2004). Due to the merging of new diseases and resistance development to many drugs, plant-based products are the best choice for discovering new promising agents (Khan et al., 2019) (Piscopo et al., 2020).

Interestingly, diverse bioactive secondary metabolites support the traditional use of *D. cinnabari* for treating many diseases. This is the first study to report molecular docking of *D. cinnabari* secondary metabolites with different targets protein from the dengue virus and *Ae. agypti*. Our study revealed that the selected bioactive molecules could efficiently bind to the targeted receptors, and molecular docking can be effectively used in finding promising inhibitors from *D. cinnabari* extract. The higher negative docking score signified a high binding affinity between the receptor (target protein) and ligand, indicating the higher efficacy of bioactive molecules. In the present investigation, beta-Sitosterol and stigmasterol are the lead compounds showing the highest docking score among the bioactive compounds. The best-docked ligand scores for dengue virus was 4V0Q (stigmasterol, −9.0), whereas the best-docked ligand scores for *Ae. agypti* was recorded for 1PZ4 (beta-Sitosterol, −9.9).

An effective drug for DENV infection is required to reduce the DENV infection. It is a challenge to find a good drug candidate (Marnolia et al., 2018). The Dengue NS5 methyltransferase is an important nonstructural protein (104 kDa), a component of viral replication complex, that has enzymatic activities, and the important drug target for antiviral discovery (Yin et al., 2009). It contains both RNA-dependent RNA polymerase and methyltransferase (Marnolia et al., 2018).

AeSCP-2 is an essential gene for the development and survival of mosquitoes(Spates et al., 1988). Searching for *Ae. agypti* AeSCP-2 inhibitors is a way to find a compound that could be employed in mosquito control. Therefore, If the carrier protein AeSCP-2 is blocked, it would disrupt the cholesterol uptake and cause mosquito larval death (Kim et al., 2005). Targeting cholesterol metabolism to control the mosquito population is one of the aims of diseases causing vector management.

Different compounds can be used as inhibitors for treating DENV infection and as a larvidical agent. One of them is phytosterols. Phytosterols are a large group of compounds with various biological activities. Among phytosterols, β-sitosterol, campesterol, and stigmasterol are the major compounds found with a high percentage in plants. β-sitosterol and stigmasterol are a nutritional complement with a long history of use as a pharmaceutical products (Paniagua-Pérez et al., 2005). Many scientific reports recognized that they possess anxiolytic, antinociceptive and sedative effects, immunomodulatory, anti-inflammatory, antimicrobial, anticancer, hepatoprotective, lipid-lowering effect, wound healing effect, antidiabetic, and antioxidant, larvicidal, neuroprotective, antibaceterial activities (Fraile et al., 2012, Dighe et al., 2016, Sharmila and Sindhu 2017) (Ododo et al., 2016) (Sharmila and Sindhu 2017) (Abdou et al., 2019), (Yuan et al., 2019) (Park et al., 2019) (Park et al., 2019) (Ponnulakshmi et al., 2019) (Ghosh 2013) (Sultana and Khalid 2010) (Alawode et al., 2021).

Computational chemistry results positively correlated with the previous in vitro studies where stigmasterol (Gade et al., 2017) and β-sitosterol (Ghosh 2013) compounds were very effective against *Ae. agypti*. For instance, the β-sitosterol isolated from *Abutilon indicum* extract exhibited an LC_{50} value of 11.5 mg/L against *Ae. egypti* and LC_{50} value of 26.7 mg/L against *Anopheles stephensi* (Abdul Rahuman et al., 2008). *Similarly, Cestrum diurnum* extract was reported for its toxicity against *Culex quinquefasciatus (*Ghosh et al., 2008*)*. Our result also correlated with the reported studies in which the ethyl acetate (EtOAc) extract of *Melochia umbellata* (stem bark) inhibited the dengue virus (DENV-2) with an IC_{50} value of 2.81 μg/mL (Soekamto et al., 2018). In the same way, stigmasterol isolated from the EtOAc extract of *M. umbellata* inhibited DENV-2 with IC_{50} values of 9.11 μg/mL (Soekamto et al., 2019).

The present investigation focused on identifying different secondary metabolites from *D. cinnabari* using GC–MS analysis. The bioactive compounds identified are responsible for various pharmacological activities. The compounds stigmasterol and β-sitosterol showed promising binding affinity against the selected target proteins in the molecular docking studies. From our investigations, *D. cinnabari* may enable us to develop promising drugs against various infections. Despite the effectiveness of computational chemistry (in silico studies), the main limitation is the lack of confidence on the ability of scoring functions to give precise binding energies Therefore, in vivo and in vitro investigations are needed to support the results of silico studies.

Declaration of Competing Interest

The authors declare that they have no known competing financial interests or personal relationships that could have appeared to influence the work reported in this paper.

Acknowledgement

Researchers Supporting Project number (RSP2022R414), King Saud University, Riyadh, Saudi Arabia.

References

Abdou, E.M., Fayed, M.A., Helal, D., et al., 2019. Assessment of the hepatoprotective effect of developed lipid-polymer hybrid nanoparticles (LPHNPs) encapsulating naturally extracted β-Sitosterol against CCl_4 induced hepatotoxicity in rats. Sci. Rep. 9 (1), 1–14.

Abdul Rahuman, A., Gopalakrishnan, G., Venkatesan, P., et al., 2008. Isolation and identification of mosquito larvicidal compound from *Abutilon indicum* (Linn.) Sweet. Parasitol. Res. 102 (5), 981–988.

Adams, R. P., 2007. Identification of essential oil components by gas chromatography/mass spectrometry, Allured publishing corporation Carol Stream.

Alawode, T.T., Lajide, L., Olaleye, M., et al., 2021. Stigmasterol and β-Sitosterol: Antimicrobial Compounds in the Leaves of *Icacina trichantha* identified by GC–MS. Beni-Suef University Journal of Basic and Applied Sciences. 10 (1), 1–8.

Al-Awthan, Y. S. and O. S. Bahattab, 2021. Phytochemistry and Pharmacological Activities of *Dracaena cinnabari* Resin. BioMed Research International. Volume 2021 | Article ID 8561696 | https://doi.org/10.1155/2021/8561696.

Al-Awthan, Y.S., Zarga, M.A., Abdalla, S., 2010. Flavonoids content of *Dracaena cinnabari* resin and effects of the aqueous extract on isolated smooth muscle preparations, Perfused heart, blood pressure and Diuresis in the rat. Jordan J Pharm Sci. 3 (1), 8–16.

Al-Fatimi, M., 2018. Ethnobotanical survey of *Dracaena cinnabari* and investigation of the pharmacognostical properties, antifungal and antioxidant activity of its resin. Plants. 7 (4), 91.

Baumer, U., Dietemann, P., 2010. Identification and differentiation of dragon's blood in works of art using gas chromatography/mass spectrometry. Anal. Bioanal. Chem. 397 (3), 1363–1376.

Benelli, G., 2015. Research in mosquito control: current challenges for a brighter future. Parasitol. Res. 114 (8), 2801–2805.

Dighe, S.B., Kuchekar, B., Wankhede, S., 2016. Analgesic and anti-inflammatory activity of β-sitosterol isolated from leaves of *Oxalis corniculata*. Int J of Pharmc Res. 6 (3), 109–113.

Fraile, L., Crisci, E., Córdoba, L., et al., 2012. Immunomodulatory properties of beta-sitosterol in pig immune responses. Int. Immunopharmacol. 13 (3), 316–321.

Gade, S., Rajamanikyam, M., Vadlapudi, V., et al., 2017. Acetylcholinesterase inhibitory activity of stigmasterol & hexacosanol is responsible for larvicidal and repellent properties of Chromolaena odorata. Biochimica et Biophysica Acta (BBA)-General Subjects. 1861 (3), 541–550.

Geris, R., Ribeiro, P.R., Brandão, M.D.S., et al., 2012. Bioactive natural products as potential candidates to control Aedes aegypti, the vector of dengue. Stud. Nat. Prod. Chem. 37, 277–376.

Ghosh, A., 2013. Efficacy of phytosterol as mosquito larvicide. Asian Pacific Journal of Tropical Disease. 3 (3), 252.

Ghosh, A., Chowdhury, N., Chandra, G., 2008. Laboratory evaluation of a phytosteroid compound of mature leaves of Day Jasmine (Solanaceae: Solanales) against larvae of *Culex quinquefasciatus* (Diptera: Culicidae) and nontarget organisms. Parasitol. Res. 103 (2), 271–277.

Goldenthal, K., K. Midthun and K. Zoon, 1996. Chapter 51: Control of viral infections and diseases. Medical Microbiology. 4th ed. Galveston, TX: University of Texas Medical Branch; 1996. Available from: https://www.ncbi.nlm.nih.gov/books/NBK8492/. [Last accessed on 2022 May 5].

Khan, T., Ali, M., Khan, A., et al., 2019. Anticancer plants: A review of the active phytochemicals, applications in animal models, and regulatory aspects. Biomolecules 10 (1), 47.

Kim, M.-S., Wessely, V., Lan, Q., 2005. Identification of mosquito sterol carrier protein-2 inhibitors. J. Lipid Res. 46 (4), 650–657.

Kitchen, D.B., Decornez, H., Furr, J.R., et al., 2004. Docking and scoring in virtual screening for drug discovery: methods and applications. Nat. Rev. Drug Discov. 3 (11), 935–949.
Lounkine, E., Keiser, M.J., Whitebread, S., et al., 2012. Large-scale prediction and testing of drug activity on side-effect targets. Nature 486 (7403), 361–367.
Magden, J., Kääriäinen, L., Ahola, T., 2005. Inhibitors of virus replication: recent developments and prospects. Appl. Microbiol. Biotechnol. 66 (6), 612–621.
Marnolia, A., E. Toepak, S. Siregar, et al., 2018. Computational screening of flavonoid based inhibitor targeting DENV NS5 methyltransferase. AIP Conference Proceedings, AIP Publishing LLC. (Vol. 2023, No. 1, p. 020070).
McLafferty, F.W., Stauffer, D.B., 1989. The Wiley/NBS registry of mass spectral data. Wiley, New York.
Messina, J.P., Brady, O.J., Golding, N., et al., 2019. The current and future global distribution and population at risk of dengue. Nat. Microbiol. 4 (9), 1508–1515.
Ododo, M.M., Choudhury, M.K., Dekebo, A.H., 2016. Structure elucidation of β-sitosterol with antibacterial activity from the root bark of *Malva parviflora*. Springerplus 5 (1), 1–11.
Paniagua-Pérez, R., Madrigal-Bujaidar, E., Reyes-Cadena, S., et al., 2005. Genotoxic and cytotoxic studies of beta-sitosterol and pteropodine in mouse. J. Biomed. Biotechnol. 2005 (3), 242–247.
Park, Y.J., Bang, I.J., Jeong, M.H., et al., 2019. Effects of β-Sitosterol from corn silk on TGF-β1-induced epithelial–mesenchymal transition in lung alveolar epithelial cells. J. Agric. Food Chem. 67 (35), 9789–9795.
Piscopo, M., Tenore, G.C., Notariale, R., et al., 2020. Antimicrobial and antioxidant activity of proteins from *Feijoa sellowiana* Berg. fruit before and after in vitro gastrointestinal digestion. Nat. Prod. Res. 34 (18), 2607–2611.
Ponnulakshmi, R., Shyamaladevi, B., Vijayalakshmi, P., et al., 2019. In silico and in vivo analysis to identify the antidiabetic activity of beta sitosterol in adipose tissue of high fat diet and sucrose induced type-2 diabetic experimental rats. Toxicol. Mech. Methods 29 (4), 276–290.
Sami, M., Rowaida, B., Hafiz, A., et al., 2021. The epidemiology and incidence of dengue in Makkah, Saudi Arabia, during 2017–2019. Saudi Med. J. 42 (11), 1173–1179.
Seo, S.-M., Park, H.-M., Park, I.-K., 2012. Larvicidal activity of ajowan (Trachyspermum ammi) and Peru balsam (Myroxylon pereira) oils and blends of their constituents against mosquito, *Aedes aegypti*, acute toxicity on water flea, *Daphnia magna*, and aqueous residue. J. Agric. Food Chem. 60 (23), 5909–5914.
Sharmila, R., Sindhu, G., 2017. Evaluate the Antigenotoxicity and anticancer role of β-Sitosterol by determining oxidative DNA damage and the expression of phosphorylated mitogen-activated protein Kinases', C-fos, C-Jun, and endothelial growth factor receptor. Pharmacogn. Mag. 13 (49), 95.
Soekamto, N. H., S. Liong, S. Fauziah, et al., 2018. Dengue antiviral activity of polar extract from *Melochia umbellata* (Houtt) Stapf var. Visenia. Journal of Physics: Conference Series, IOP Publishing. (Vol. 979, No. 1, p. 012017).
Soekamto, N., F. Ahmad and F. Appa, 2019. Potential of stigmasterol from EtOAc extract *Melochia umbellata* (Houtt) Stapf var. Visenia as Dengue Antivirus. Journal of Physics: Conference Series, IOP Publishing. (Vol. 1341, No. 3, p. 032044).
Spates, G., Deloach, J., Chen, A., 1988. Ingestion, utilization and excretion of blood meal sterols by the stable fly, *Stomoxys calcitrans*. J. Insect Physiol. 34 (11), 1055–1061.
Sultana, N., Khalid, A., 2010. Phytochemical and enzyme inhibitory studies on indigenous medicinal plant *Rhazya stricta*. Nat. Prod. Res. 24 (4), 305–314.
WHO, (10 January 2022). "Dengue and severe dengue". https://www.who.int/news-room/fact-sheets/detail/dengue-and-severe-dengue (accessed 20/9/20222).
Williams, D.H., Stone, M.J., Hauck, P.R., et al., 1989. Why are secondary metabolites (natural products) biosynthesized. J. Nat. Prod. 52 (6), 1189–1208.
Xin, N., Li, Y.-J., Li, Y., et al., 2011. Dragon's Blood extract has antithrombotic properties, affecting platelet aggregation functions and anticoagulation activities. J. Ethnopharmacol. 135 (2), 510–514.
Yin, Z., Chen, Y.-L., Schul, W., et al., 2009. An adenosine nucleoside inhibitor of dengue virus. Proc. Natl. Acad. Sci. 106 (48), 20435–20439.
Ying, L., Hao-Fu, D., Hui, W., et al., 2011. Chemical constituents from dragon's blood of *Dracaena cambodiana*. Chin. J. Nat. Med. 9 (2), 112–114.
Yuan, C., Zhang, X., Long, X., et al., 2019. Effect of β-sitosterol self-microemulsion and β-sitosterol ester with linoleic acid on lipid-lowering in hyperlipidemic mice. Lipids Health Dis. 18 (1), 1–11.